Chemistry & Biology
Article

A Fluorescent Probe for the Detection of Myeloperoxidase Activity in Atherosclerosis-Associated Macrophages

Joanna Shepherd,[1,4] Scott A. Hilderbrand,[2,4] Peter Waterman,[2] Jay W. Heinecke,[3] Ralph Weissleder,[2] and Peter Libby[1,*]
[1]Department of Medicine, Cardiovascular Division, Brigham and Women's Hospital, Harvard Medical School, Boston, MA 02215, USA
[2]Center for Molecular Imaging Research, Massachusetts General Hospital and Harvard Medical School, Charlestown, MA 02129, USA
[3]Department of Medicine, University of Washington, Seattle, WA 98195, USA
[4]These authors contributed equally to this work.
*Correspondence: plibby@rics.bwh.harvard.edu
DOI 10.1016/j.chembiol.2007.10.005

SUMMARY

The myeloperoxidase (MPO)-derived oxidant hypochlorous acid (HOCl/OCl^-) is implicated in the pathogenesis of atherosclerosis and other inflammatory states. We have synthesized an imaging probe, sulfonaphthoaminophenyl fluorescein (SNAPF), that selectively reacts with HOCl. SNAPF detects HOCl produced by stimulated MPO-expressing cells cultured from human whole blood, as well as HOCl from bone marrow (BM)-derived macrophages isolated from transgenic mice that express human MPO. Two lines of evidence indicate that SNAPF permits the in vivo imaging of HOCl production. First, we used this approach to demonstrate HOCl production by neutrophils in experimental murine peritonitis. Second, we detected HOCl production by MPO expressing cells in human atherosclerotic arteries. Thus, fluorescence reflectance imaging by SNAPF may provide a valuable noninvasive molecular imaging tool for implicating HOCl and MPO in the damage of inflamed tissues.

INTRODUCTION

Oxidative stress likely participates in the pathogenesis of diseases as diverse as cancer [1], those that affect the lungs [2], and skin disease [3]. Oxidative processes in tissues can involve Fenton reactions, in which free metal ions (most commonly, Fe^{2+}) interact with peroxide to yield oxidizing products such as the hydroxyl radical and superoxide [4–6]. An alternative pathway for the production of oxidizing agents, independent of Fenton chemistry, involves the action of myeloperoxidase (MPO). MPO is a heme enzyme secreted in large amounts by activated neutrophils along with superoxide. Superoxide dismutates spontaneously or enzymatically to hydrogen peroxide, a relatively unreactive oxidant, which is then used as a substrate by MPO to produce hypochlorous acid (HOCl) [7]. With a pK_a of 7.463 at 35° [8], under physiological conditions, approximately half of the HOCl dissociates to the hypochlorite anion (OCl^-), one of the most powerful natural oxidants. Hypochlorite likely functions to injure microorganisms oxidatively; however, it can also have detrimental effects on host tissue. Neutrophil derived HOCl has been implicated in lung injury [9–11], rheumatoid arthritis [12, 13], hepatic ischemia-reperfusion injury [14], and renal disease [15, 16] among others.

Oxidative stress within the vasculature plays multiple roles in the development of atherosclerosis, particularly with regard to oxidative modifications of lipoproteins [17]. Monocytes and neutrophils, cells that do not accumulate appreciably in atherosclerotic plaques, typically contain high levels of MPO. Yet, a subset of monocyte-derived macrophages in human atheromatous lesions retain MPO [18]. These MPO^+ macrophages colocalize with hypochlorite-modified proteins [19]. Furthermore, human atherosclerotic plaques harbor 3-chlorotyrosine, a product of MPO-mediated reactions [20]. Conversely, murine macrophages from sites of atherosclerotic plaques do not contain immunoreactive MPO or 3-chlorotyrosine [21], making mice an inappropriate model for investigating the role of macrophage-derived MPO in the pathogenesis of disease. This limitation has recently been circumvented by the creation of transgenic mice that express human MPO, h-MPOTg [22]. Irradiated LDL-receptor-deficient ($LDLR^{-/-}$) animals receiving bone marrow from transgenic animals develop accelerated atherosclerosis during hypercholesterolemia when compared to those with wild-type donors. MPO resides within plaques from the transgenic, but not wild-type, BM recipients. Moreover, elevated levels of plasma MPO independently predict risk for coronary events and myocardial infarction in clinical studies [23–25].

Within the context of cardiovascular disease, the effects of HOCl on tissue are numerous. For example, hypochlorite can cause endothelial cell (EC) apoptosis, a process during which the dying ECs release tissue factors that

may contribute to thrombosis [26]. Hypochlorite can derivatize both low- and high-density lipoproteins. Along with numerous other oxidants, it oxidizes LDL to OxLDL, a proatherogenic form that readily enters macrophages, thus promoting foam cell formation in early lesion development [27–29]. Oxidized LDL has chemotactic activity [30–32] and is immunogenic [33, 34]. Hypochlorite oxidizes tyrosine 192 on apo-A1, the major protein of HDL [35]. This oxidation impairs cholesterol transport via the cell membrane transporter ATP binding cassette transporter A1 (ABCA-1) [36, 37].

To study the contribution of oxidative species to disease processes, a number of fluorescent probes have been developed. Most detect multiple reactive oxygen species (ROS) and can be prone to auto-oxidation. It is likely that different ROS play distinct roles in specific pathological processes, hence methods for selective detection of specific ROS are desirable. To this end, Setsukinai et al. [38] developed two novel auto-oxidation resistant fluoroscein-based probes, 2-[6-(4′-hydroxy)phenoxy-3H-xanthen-3-on-9-yl]benzoic acid (APF) and 2-[6-(4′-amino) phenoxy-3H-xanthen-3-on-9-yl]benzoic acid (HPF), which detect only the highly reactive oxygen species (hROS) hydroxyl radical (OH·), peroxynitrite ($ONOO^-$), and HOCl. Furthermore, because APF but not HPF detects HOCl, use of the two probes in tandem might distinguish HOCl presence from other hROS.

Modification of the APF probe to render it detectable with longer emission wavelengths would increase its suitability for bioimaging since lipids and hemoglobin within normal tissue absorb light within the visible light range (which includes the emission spectrum of fluorescein, ~520 nm). In particular, elastin produces strong green autofluorescence in arteries, rendering probes that emit in the green range unsuitable for atherosclerosis research. The absorption coefficient of tissue components is lowest in the far red/near infra red (NIR) range from approximately 650–900 nm [39]. In this work, development of a water-soluble probe for hypochlorite, SNAPF, which has maximal excitation and emission wavelengths of 614 and 676 nm, respectively, is reported.

The current study investigated the utility of SNAPF as a sensor for the detection of HOCl-generating MPO positive cells and, thus, probable oxidative stress-related damage, in inflammatory states. We demonstrate that SNAPF detects HOCl formation after stimulation of human neutrophils, MPO-containing human macrophages, and transgenic mouse macrophages that express human MPO. In addition, we demonstrate the ability of SNAPF to detect HOCl generation in vivo, and consequently to potentially directly implicate HOCl-mediated tissue injury in inflammation in a noninvasive manner by using fluorescence reflectance imaging (FRI).

RESULTS

SNAPF Probe Synthesis and Characterization

In an effort to prepare a water-soluble far-red or NIR probe for hypochlorite, a xanthene-based dye scaffold was chosen. This allowed for the preparation of red-shifted hypochlorite sensors based on an activation strategy similar to that reported for APF, where oxidative cleavage of a 4-aminophenylether modified fluorescein, which has quenched fluorescence, results in generation of free fluorescein with strong fluorescence emission. SNAPF is prepared in a three-step process from sulfonaphthofluorescein, **1**, as detailed in Figure 1A. The 4-nitrophenyl modified intermediate **2** was prepared in moderate yield by nucleophilic attack of dye **1** on 1-fluoro-4-nitrobenzene in the presence of sodium carbonate. The nitro group of **2** is then reduced with hydrogen gas in the presence of palladium on carbon catalyst to yield crude SNAPF. During the course of this reduction, a significant amount of free dye **1** is generated. Dye **1** and SNAPF have nearly identical retention times by HPLC and cannot be resolved easily. To facilitate isolation of pure SNAPF, the crude reduction product was protected with BOC anhydride. This enabled easy separation of the mono- and di-BOC functionalized SNAPF derivatives, **3a** and **3b**, respectively, by preparative HPLC. Purified SNAPF is then isolated by treatment of **3a** and **3b** with a methanolic solution of TFA.

As with APF, the reaction of SNAPF with strong oxidants results in oxidative cleavage of the 4-aminophenyl moiety, generating highly fluorescent free dye **1** (Figure 1B). Treatment of SNAPF with excess HOCl in PBS results in a greater than 8-fold increase in fluorescence emission (Figure 1C), which corresponds to generation of **1**. Once generated, deprotonated dye **1** has an absorption maximum at 614 nm and emission at 676 nm [40].

SNAPF Detects Chemically and Enzymatically Generated HOCl In Vitro

To establish which oxidative species SNAPF reports, we exposed 10 μM SNAPF solutions to a range of chemically generated oxidants (Figure 2A). Of the oxidants tested, a significant increase in fluorescence occurs only with HOCl, indicating the selectivity of SNAPF for hypochlorite. In addition, the fluorescence emission of activated SNAPF after exposure to HOCl increases in a concentration-dependent manner (Figure 2B).

SNAPF can also detect HOCl generated by purified MPO, after incubation with the enzyme at 37°C for 30 min. As expected, the probe (at 10 μM) does not detect generation of HOCl in this system in the absence of the required MPO substrate, H_2O_2 (Figure 2C). Preincubation of the enzyme with 5 μM MPO inhibitor (4-aminobenzoic acid hydrazide) before the addition of 2 μM H_2O_2, ablated signal generation, although the inhibitor is not effective when added after the peroxide, presumably due to the high rate of HOCl generation. The MPO inhibitor similarly affected detection of HOCl by APF (data not shown).

SNAPF Detects HOCl Generated by Stimulated Human Neutrophils

Since MPO is expressed at high levels by neutrophils, we wished to establish first whether SNAPF could detect HOCl generation by these cells following activation with PMA. Freshly isolated neutrophils incubated with 10 μM

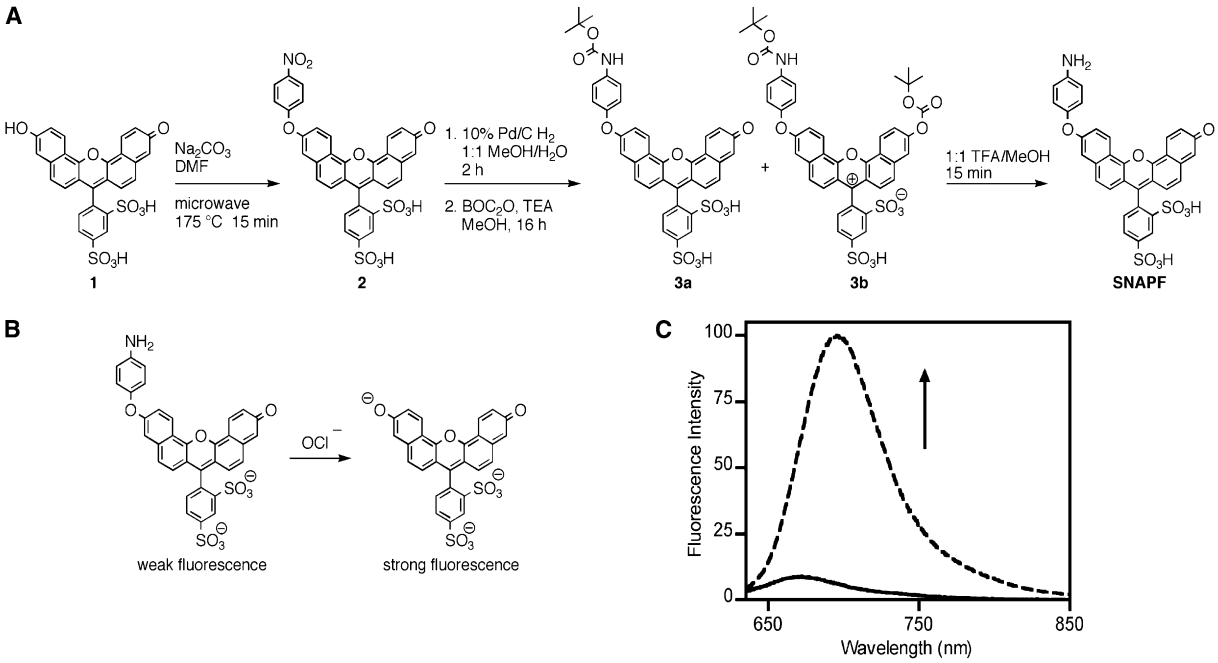

Figure 1. Synthesis of SNAPF

(A) Synthesis of SNAPF.

(B) Activation of SNAPF.

(C) Fluorescence emission traces, exciting with 625 nm light, of SNAPF before (solid line) and after (dashed line) exposure to excess sodium hypochlorite in PBS (pH 7.4) at room temperature for 5 min.

SNAPF (or SNAPF + 2 μM MPO inhibitor) were stimulated with PMA at a concentration of 400 nM in the buffer and monitored by fluorescence spectrophotometry. The fluorescent signal from the activated probe rapidly increased following cell stimulation and reached a peak around 90 min poststimulation after which it appeared to remain stable (Figure 3A). The fluorescence increase quantified with the plate reader translated well to fluorescence microscopy; neutrophils incubated with SNAPF were visibly brighter following PMA stimulation (Figures 3B and 3C). In both quantitative and qualitative data sets, coincubation of the neutrophils with MPO inhibitor ablated the fluorescence of SNAPF following cell stimulation (Figures 3A and 3D). Coincubation with MPO inhibitor at a final concentration of 2 μM was found to be sufficient to diminish the fluorescent signal.

SNAPF Detects HOCl Generated from Stimulated Murine Macrophages Transgenic for Human MPO

As noted above, mouse macrophages do not express MPO. Therefore, to examine whether SNAPF can detect HOCl generated by stimulation of MPO-containing macrophages, we first isolated and cultured bone marrow-derived macrophages, by using standard techniques, from mice transgenic for human MPO with age-matched wild-type mice as controls. Reverse transcriptase amplification of cDNA reveals transcription of the hMPO gene in h-MPOTg, but not WT, mice (Figure 4A). The translated protein is enzymatically active (Figure 4B). Fluorescence readings of stimulated h-MPOTg and WT BM-derived macrophages coincubated with probe taken over a 90 min time period show a ~25% increase in h-MPOTg cell fluorescence that peaks around 15 min poststimulation and reaches a statistically significant difference from WT cells by 75 min poststimulation (Figure 4C). h-MPOTg or WT macrophages cultured in 96-well plates were also used to demonstrate visually the poststimulation increase in fluorescence observed with the plate readers via fluorescence microscopy. h-MPOTg, but not WT, macrophages show an increase in fluorescence following stimulation abrogated by coincubation with 2 μM MPO inhibitor (Figures 5A–5F).

SNAPF Identifies HOCl Generated from Stimulated Human MPO-Containing Macrophages

To study whether SNAPF can detect HOCl generated by stimulation of MPO+ human macrophages, human monocytes were isolated from whole blood and then cultured to either the MPO-expressing phenotype (MPOhi, cultured in serum free media with addition of GM-CSF [26]) or as classical macrophages (MPOlo). MPOlo cells do not contain any MPO protein as previously shown by western blotting [26]. MPOhi cells contain enzymatically active MPO that produce HOCl after stimulation of the cells with PMA as measured by the oxidation of TNB to DTNB in a taurine-containing buffer (Figure 4B). Unstimulated MPOhi cells do not demonstrate HOCl release (data not shown).

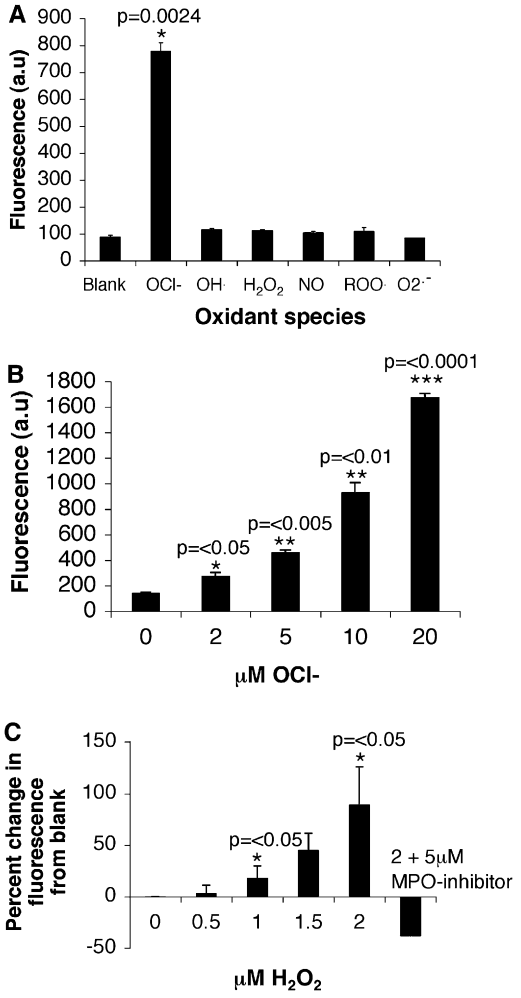

Figure 2. Fluorescence Response of SNAPF after Activation

(A) SNAPF selectively detects HOCl when reacted against a panel of biological oxidants. All oxidants are 100 μM except HOCl, which is 10 μM, and were generated as described previously [38] (n = 3).

(B) Briefly, increasing concentrations of native HOCl result in an increase in SNAPF-generated fluorescence (n = 3).

(C) Purified MPO, 11.2 nM, generates increasing amounts of SNAPF-detectable HOCl when higher amounts of H_2O_2 are added as substrate. Fluorescence generated by addition of 2 μM H_2O_2 is ablated by coincubation of MPO with a selective MPO inhibitor at a final concentration of 5 μM (n = 3). Error bars represent the SEM.

We performed a time-course analysis of cells stimulated with PMA at a final concentration of 400 nM by using a fluorescent plate reader and achieved results similar to those for h-MPOTg macrophages (Figure 4D). In this case, fluorescence emission from the activated probe in MPOhi cells peaked at around 60 min poststimulation, although the fluorescence signal was statistically different from WT fluorescence earlier in the time course, at 15–30 min poststimulation. The increase in fluorescence was also imaged after stimulation of human MPOhi and MPOlo cells by fluorescence microscopy, and again results comparable to those from the mouse experiments were found (Figures 5G–5L).

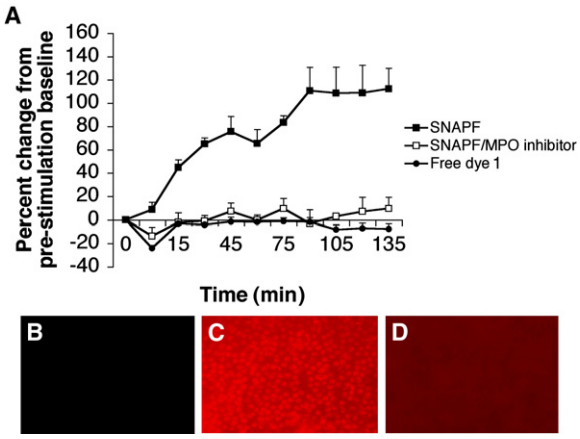

Figure 3. SNAPF Detects HOCl Generated by Stimulated Human Neutrophils

SNAPF, coincubated with neutrophils isolated from fresh venous blood, fluoresces after stimulation of the neutrophils with 400 nM PMA. The fluorescence emission is quantifiable on a plate reader (A, data points represent the mean + SEM, n = 3), and the increase in fluorescence is sufficient to permit imaging by fluorescence microscopy (B–D). Neutrophils coincubated with SNAPF pre- (B) and poststimulation (C) with PMA. The increase in fluorescence post stimulation is attenuated by coincubation with 2 μM MPO inhibitor (A and D) (n = 4).

SNAPF Detects HOCl Generation In Vivo

We first determined whether the increase in fluorescence of activated SNAPF could be distinguished by FRI in vitro. Incubation of 10 μM SNAPF with 20 μM HOCl at 37°C for 30 min results in a 7-fold increase in fluorescence of the probe as detected by FRI (Figure 6A). Given this result, we subsequently injected the probe (50 nmoles) into h-MPOTg mice that had peritonitis induced by thioglycollate. Thioglycollate was injected 24 hr before probe administration, providing an expected mix of about 60% neutrophils and 40% monocytes/macrophages in the peritoneal inflammatory milieu[2]. When SNAPF was injected i.p., a 1.4-fold increase in fluorescence of the peritoneum in vivo is observed after 1 hr (Figures 6B–6D). Fluorescence emission did not increase when SNAPF was injected into control mice, nor did fluorescence increase in animals with peritonitis and control mice when dye **1** is used as a control in place of SNAPF (Figure 6B).

SNAPF Detects HOCl in Human Atherosclerotic Plaque

Having established that the probe can detect MPO activity in isolated cells and in whole animals in vivo, we determined whether we could use SNAPF to provide direct evidence of HOCl in human atherosclerotic plaque. Frozen sections of atherosclerotic human carotid arteries yielded SNAPF-derived fluorescence. This fluorescence is distinct from autofluorescence visible through the FITC filter set (Figures 7A–7C). Subsequent immunohistochemical staining of parallel sections colocalized both macrophages and MPO with the fluorescent areas (Figures 7D and 7E). SNAPF was also incubated with thinly sliced

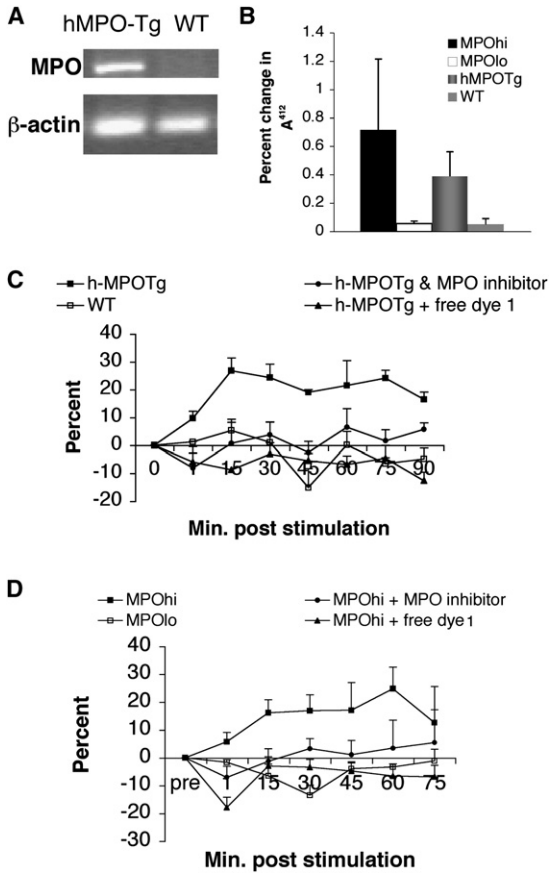

Figure 4. MPO+ Macrophages Contain Active MPO that Generates HOCl Detectable by SNAPF, Following Stimulation

(A) The gene for hMPO is transcribed in bone marrow-derived macrophages from hMPO-Tg, but not WT, mice as demonstrated by RT-PCR.

(B) This is translated into functionally active MPO, established by a dTNB assay. Results are expressed as a percentage decrease in absorbance at 412 nm per μg protein (n = 3). Enzymatically active MPO is also present in human MPOhi cells (B) (n = 4).

(C and D) HOCl generated by hMPO-Tg BM macrophages (C) (n = 3) or human MPOhi macrophages (D) (n = 5) is quantifiably detected by SNAPF with a fluorescent plate reader, following cell stimulation with 400 nM PMA. Results are expressed as a percentage change in fluorescence from baseline readings (prestimulation) over time. Data points represent the mean + SEM.

(~1 mm thick) sections of freshly excised atheromatous carotid arteries and again showed highly fluorescent regions on fluorescence microscopy, suggesting probe activation (Figures 7E–7G). Following imaging, the sections were frozen in OCT and sectioned to 6 μm thick slices. Immunohistochemistry demonstrated the presence of MPO+ cells and macrophages within the samples (Figures 7H and 7I).

DISCUSSION

Oxidative stress has far reaching effects within living tissue. We now understand that not all biological oxidants behave in the same manner in, or have equivalent effects on, cells and tissues. Tools that report the distinct roles of different oxidant species in disease processes would help unravel pathophysiologic mechanisms and might ultimately furnish insight enabling the development and evaluation of more targeted therapies. MPO produces a number of oxidants, one of which is HOCl. To distinguish the action of HOCl from other oxidants, as we become increasingly aware of the multiplicity of its effects on tissue components, would provide valuable insights into oxidative mechanisms in diverse diseases. The SNAPF probe described in this work can selectively detect HOCl, including that generated by purified MPO. No other fluorescent probe thus far has shown such high specificity for HOCl over other biologically relevant oxidants, although the prior sensors, HPF and APF, might be used in tandem to distinguish HOCl from hydroxyl radical and peroxynitrite. SNAPF obviates the need for dual probes in the detection of HOCl. In addition SNAPF has absorption and fluorescence emission maxima in the far red, which maximizes tissue penetration and minimizes the potential of interference from tissue autofluorescence, a particular concern in the study of elastin-rich arterial tissues. We demonstrated that SNAPF can detect HOCl generated from stimulated human neutrophils, the classic source of MPO. Thus, this probe could serve as a valuable tool for investigation of multiple disease states characterized by acute inflammation involving infiltration of polymorphonuclear monocytes.

In our experiments, human and murine MPO+ macrophages appear to generate sufficient HOCl after stimulation with PMA to be detected by SNAPF, both quantitatively and qualitatively. Although PMA is not a physiologically relevant stimulus in the context of atheroma, HOCl production in MPOhi macrophages is expected following cell activation by stimulants present within an atherosclerotic lesion, such as CD40L and cholesterol crystals [41]. This study aimed to determine whether SNAPF could detect HOCl generated from living cells; for this purpose, stimulation with PMA was appropriate as our previous studies showed that MPOhi cells stimulated with PMA generate substantial HOCl. A study using an alternative stimulus, N-formyl-methionylleucylphenylalanine (FMLP), demonstrated that stimulation of human neutrophils preincubated with tumor necrosis factor-α resulted in rapid accumulation of HOCl over the first 30 min of stimulation, reaching a maximum concentration approximately 60 min poststimulation [42]. Fluorescence time course data using SNAPF to detect HOCl also suggests a rapid generation of HOCl following cell stimulation, with comparable times for maximum concentration reached (60–75 min for macrophages, 90 min for neutrophils).

Since degranulation of certain leukocytes following stimulation releases preformed MPO, we may expect the extracellular milieu to become highly fluorescent when cells are incubated with SNAPF. Instead, we see enhanced fluorescence of cells themselves, in agreement with the previous data from Setsukinai et al., who demonstrated increased fluorescence of porcine neutrophils incubated with APF following stimulation [38]. The reasons

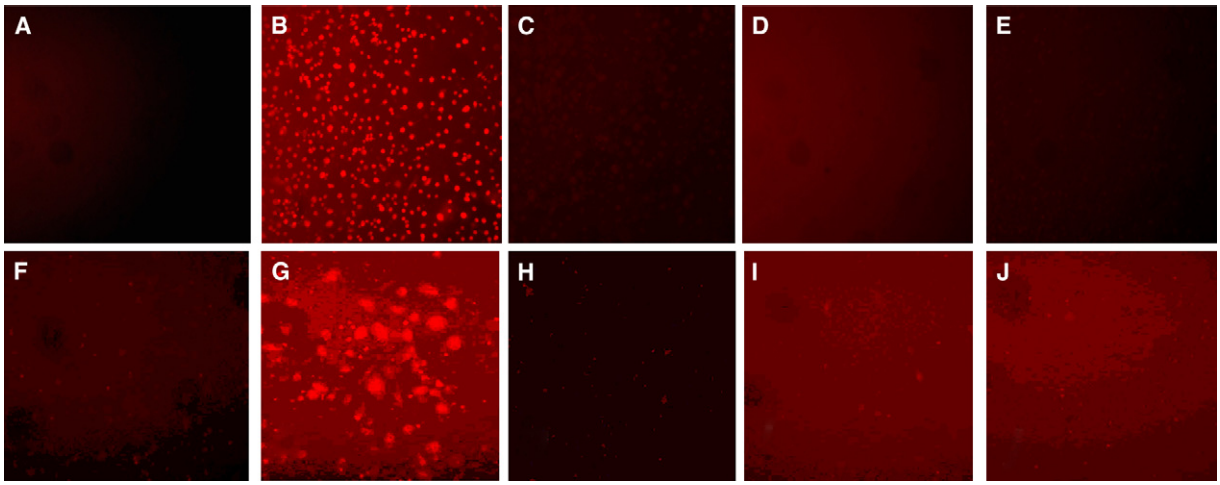

Figure 5. SNAPF Is Activated upon Incubation with MPO+ Macrophages Stimulated with PMA, Detectable by Fluorescence Microscopy

BM-derived macrophages from h-MPOTg and WT mice, or human MPOhi or MPOlo macrophages, were incubated with 10 μM SNAPF for 10 min prior to stimulation with 400 nM PMA. Images were acquired 30 min poststimulation with an APC filter set.

(A) h-MPOTg cells prestimulation.

(B) h-MPOTg cells poststimulation.

(C) h-MPOTg cells coincubated with 2 μM MPO inhibitor, poststimulation.

(D and E) WT cells pre- and poststimulation.

(F and G) MPOhi cells pre- and poststimulation.

(H) MPOhi cells poststimulation coincubated with MPO inhibitor.

(I and J) MPOlo cells pre- and poststimulation. Results are representative of at least three separate experiments.

for this may be twofold: the probe may be taken up into the cells by pinocytosis (as suggested for APF) and activated intracellularly by HOCl generation within phagocytic vesicles. Also, it is believed that extracellularly released HOCl is short lived and acts very locally, which may give the appearance of the macrophages or neutrophils becoming fluorescent as SNAPF is activated in close proximity to the cells.

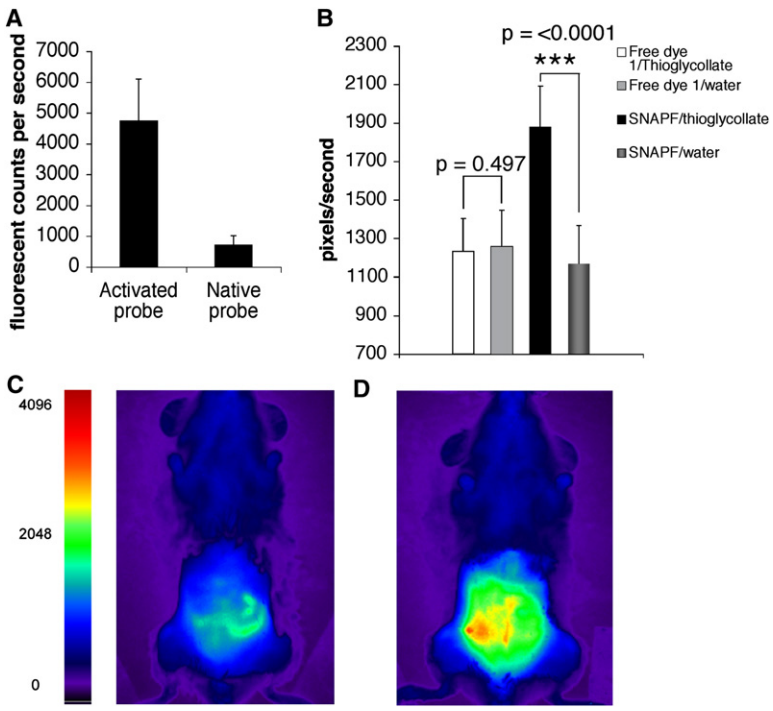

Figure 6. FRI Imaging Reveals SNAPF Activation by HOCl In Vivo

Comparison of FRI images of SNAPF alone or incubated with 20 μM HOCl shows an approximate 7-fold increase in SNAPF fluorescence in vitro by using this imaging system (A). We then injected 50 nanomoles of SNAPF i.p. into hMPO-Tg mice with thioglycollate-induced peritonitis and imaged the animals after 1 hr. There was a ~1.4-fold increase in peritoneal fluorescence (B), presumably due to contact of SNAPF with HOCl generated by activated neutrophils and macrophages present. Fluorescence was ~1.6-fold higher post-SNAPF injection in mice injected with thioglycollate as opposed to water. Error bars indicate standard deviation. (C) FRI image of h-MPOtg mouse pre-SNAPF injection; (D) the same animal postinjection of SNAPF. There was no visible fluorescence when SNAPF was injected into mice that had been injected with saline solution as opposed to thioglycollate, nor was there any increase in fluorescence of a wavelength-matched control dye, **1**, when injected into mice with peritonitis compared to saline-injected animals (B) (n = 4 per group).

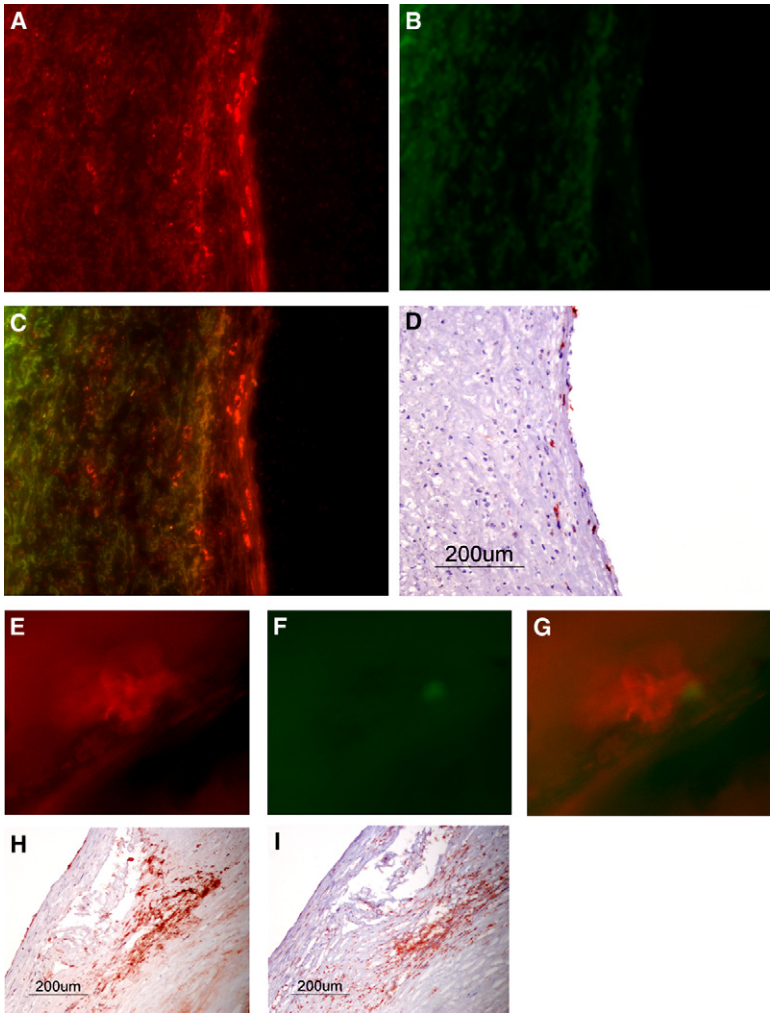

Figure 7. SNAPF Detects Areas of HOCl Generation in Frozen Sections of Human Atherosclerotic Plaque and Is Activated after Incubation with Fresh Atheromatous Carotid Endarterectomies

Frozen serial sections cut from atheromatous carotid endarterectomies (n = 4) were incubated at 37°C for 1 hr with 10 μM SNAPF, or with buffer alone as a control, and then viewed by fluorescence microscopy. Sections incubated with SNAPF were observed with an APC (A, colored in red) and a FITC (B, colored in green) filter set. Merged images (C) show that fluorescent areas with the APC filter set, which detects SNAPF, are distinct from areas that fluoresce with the FITC filter set (autofluorescence). The areas which are fluorescent with the APC filter set correspond to the location of MPO+ cells in the section (D). Freshly excised human endarterectomies (n = 4) were obtained from the operating theaters of the Brigham and Women's Hospital, cut into thin slices, and incubated with 10 μM SNAPF at 37°C for 1 hr. The slices were then viewed under a fluorescent microscope. Areas which were fluorescent when viewed with the APC filter set (E, pseudocolored in red) were not fluorescent with the FITC filter set (F, green) when exposed for the same amount of time, indicating that this was likely not autofluorescence. Merged images show distinct red colored areas (G). The slices contained MPO+ cells, established by immunohistochemical staining of adjacent tissue (H). MPO+ cells colocalized with cells, which stained positively for macrophages in adjacent sections (I).

The in vitro experiments demonstrate that SNAPF reports HOCl at concentrations as low as 2 μM. Due to the short-lived nature of HOCl, however, it is difficult to measure accurately HOCl levels in vivo. In vitro experiments have shown that 1×10^6 neutrophils/ml will generate ~43 μM HOCl 60 min after stimulation with PMA [43]. The sensitivity of SNAPF should therefore suffice to detect levels of HOCl expected even in a low-grade hypochlorite-induced oxidative state.

Results from the concurrent use of the MPO inhibitor with SNAPF in these studies suggest that the observed increases in fluorescence likely result from the specific reaction of SNAPF with MPO-derived HOCl. As an additional control for both in vivo whole-animal experiments, and in vitro cell culture work, we used sulfonaphthofluorescein, **1**, in place of SNAPF. Fluorescence emission did not increase in any of the experiments with the free dye **1**, thereby excluding activation of the naphthofluorescein itself by HOCl.

As well as cell culture-derived HOCl, SNAPF detects HOCl generation in both fresh and frozen samples of atherosclerotic human arteries and in vivo in mice with thioglycollate induced peritonitis. We believe this is the first described direct imaging evidence of HOCl within atherosclerotic plaque; previous reports have by necessity focused on the presence of HOCl-modified proteins within lesions and atheromatous vessel walls [19, 20, 36]. In its current form, SNAPF does not lend itself to in vivo imaging by intravenous injection due to the small size of the molecule. We find that in experimental peritonitis the rapid washout time of the probe makes it impractical for this purpose. Conjugation of the sensor moiety to a nonimmunogenic pegylated copolymer, a technique used in our laboratory, might evade this problem, and should be a goal of future research.

The excitation and emission wavelengths employed by SNAPF render the probe suitable for in vivo imaging, up to a tissue depth of around 1 cm. Use of these longer wavelengths circumvents difficulties found with the majority of currently available fluorescent sensors for oxidative species, which utilize shorter wavelengths [44]. Although these probes certainly have value for in vitro studies, imaging the molecular processes that occur in vivo requires imaging modalities that use fluorescent sensors less affected by normal tissue components. SNAPF could provide such a sensor.

SIGNIFICANCE

Traditional methods of visualizing vascular disease, such as angiography or ultrasound, furnish valuable tools in the evaluation of atherosclerosis. These modalities, however, have considerable limitations as they reflect anatomy or structure rather than functions or molecular processes. Too often, atherosclerosis is only diagnosed after the onset of symptoms, when the disease is already quite advanced. Preclinical diagnosis of atherosclerosis is thus a major unmet medical need. Detection of structural changes in the vasculature such as arterial calcification or stenosis may not distinguish functional aspects of plaques that correlate with their propensity to provoke thromboses, and hence clinical events such as stroke or myocardial infarction. Novel methods utilizing molecular imaging techniques can complement the more established approaches by offering a window into the dynamic biological processes such as inflammation by which a plaque may develop or become susceptible to rupture, invisible to traditional imaging techniques. Imaging techniques that report on specific disease-related molecular events, reaching beyond anatomy, may ultimately allow for the identification of vulnerable plaques before they precipitate disastrous clinical events. Such approaches could also provide much-needed tools for proof-of-concept studies and initial clinical evaluation of novel therapeutics. To this end, we have developed a novel fluorescent probe, SNAPF, which is active in the far red range of light and selectively detects HOCl, an oxidant that is implicated in many disease processes including atherosclerosis. Indeed, we have provided direct evidence of the presence of HOCl within human atherosclerotic plaque, an accomplishment previously hindered by the short half-life of the oxidant. The present results, including the use of SNAPF in a noninvasive in vivo imaging study, indicate that SNAPF could provide a valuable tool to monitor selectively the impact of HOCl on the atherogenic process, as well as other diseases, in vivo.

EXPERIMENTAL PROCEDURES

General Considerations

APF and HPF were purchased from Alexis Biochemicals, ferrous perchlorate was obtained from GFS Chemicals (Columbus, OH), and recombinant human GM-CSF and recombinant mouse G-CSF from Cell Sciences (Canton, MA). Bovine liver catalase, Krebs-Henseleit buffer, taurine, 5,5′-dithio-bis(2-nitrobenzoic acid), 3-(aminopropyl)-1-hydroxy-3-isopropyl-2-oxo-1-triazene, 10% palladium on carbon, hydrogen gas, and 1-fluoro-4-nitrobenzene were all purchased from Sigma-Aldrich (St. Louis, MO). Hydrogen peroxide was purchased from EMD Chemicals, Inc. (Gibbstown, NJ), MPO and MPO inhibitor (4-aminobenzoic acid hydrazide) from EMD Biosciences, Inc. (San Diego, CA), rabbit anti-myeloperoxidase from Biodesign (Saco, ME), and 2,2′-azobis (2-amidinopropane) dihydrochloride from Wako Chemicals USA, Inc. (Richmond, VA). Compound **1** was prepared as reported [40]. All microwave reactions were performed with a CEM (Matthews, NC) Discover LabMate microwave reactor. Preparative high performance liquid chromatography (HPLC) was performed on Varian (Palo Alto, Ca) ProStar instrument with a ProStar UV/Vis detector model 320 set at 500 nm. All HPLC data were collected with a Grace-Vydac (Columbia, MD) column, part number 218TP5210, with a flow rate of 6 ml/min, unless noted otherwise. Buffer A consisted of water and 0.1% TFA, whereas buffer B was composed of 90% acetonitrile, 9.9% water, and 0.1% TFA. Nuclear magnetic resonance spectra were acquired on a Bruker Biospin (Billerica, MA) DPX-400 spectrometer at ambient temperature and referenced to tetramethylsilane (TMS) as an internal standard. High-resolution electrospray ionization (ESI) mass spectra were collected on a Bruker Daltonics (Billerica, MA) APEXII 3 T Fourier transform mass spectrometer in the Department of Chemistry Instrumentation Facility (DCIF) at the Massachusetts Institute of Technology. Low-resolution ESI mass spectra were obtained on a ZQ mass detector from Waters Corp. (Milford, MA). Fluorescence data were collected on a Horiba Jobin Yvon (Edison, NJ) Fluorolog-3 spectrofluorometer and were corrected for the detector sensitivity.

Mice

C57BL/6J mice transgenic for human MPO (h-MPOTg) were engineered as described previously [22]. WT C57BL/6 mice were purchased from Taconic. All mice were housed in a specified pathogen free environment with 12 hr light/dark cycles and were given free access to standard chow and water. Before in vivo imaging, mice were transferred to a nonfluorescent diet (AIN-76 purified diet, Harlan) for at least 5 days.

Probe Synthesis

Intermediate **2**. To a solution of **1** (592 mg, 1.1 mmol) in 25 ml anhydrous dimethylformamide (DMF) was added sodium carbonate (424 mg, 4 mmol). The mixture was heated in an oil bath until a blue suspension was obtained. To this suspension was added 1-fluoro-4-nitrobenzene (564 mg, 4 mmol), and the reaction was heated to 175°C with a microwave reactor in a sealed reaction vessel for 15 min. Upon cooling, the excess sodium carbonate was filtered off, and the filtrate was concentrated to 5 ml by rotary evaporation. The crude product was then precipitated by addition of *tert*-butyl methyl ether (40 ml). The precipitate was isolated by centrifugation and washed with an additional portion of *tert*-butyl methyl ether (40 ml). This crude material was purified by reverse phase column chromatography with a 70 g RPC18 Isolute cartridge (Biotage, Charlottesville, VA) (eluting with: water, 0.1% TFA, and a 0 to 50% MeOH gradient in 10% increments) to afford pure **2** (285 mg, 39%) as an brown-orange solid. ^{1}H NMR (400 MHz, d_6-DMSO): δ 9.07 (1H, d, J = 8.0 Hz), 8.91 (1H, d, J = 8.0 Hz), 8.41 (1H, s), 8.36 (2H, d, J = 8.9 Hz), 8.00 (1H, d, J = 9.2 Hz), 7.91 (1H, d, J = 7.8 Hz), 7.87 (1H, d, J = 9.4 Hz), 7.73 (1H, s), 7.61 (1H, d, J = 7.8 Hz), 7.46 (2H, d, J = 8.9 Hz), 7.41 (1H, d, J = 9.2 Hz), 7.22–7.29 (4H, m). HRMS (ESI) $[M+H]^+$ calculated for $C_{33}H_{20}NO_{11}S_2^+$: 670.0472, found: 670.0455.

SNAPF

To a solution of **2** (36 mg, 0.054 mmol) in MeOH (7.6 ml) and water (0.4 ml) was added 10% palladium on carbon (10 mg). This suspension was allowed to stir under 1 atm of H_2, during which the crude product precipitated out of solution. After stirring for 2 hr, the reaction mixture was filtered through a 0.45 μ nylon filter, and the filtrate was discarded. The remaining solid was washed with 1:1 water/DMF (3 × 5 ml) giving a red solution. This solution was dried by rotary evaporation, giving crude SNAPF (8 mg) as a burgundy red solid. For purification, the crude material was BOC protected by treatment with di-*tert*-butyl dicarbonate (BOC_2O) (22 mg, 0.1 mmol) and triethylamine (TEA) (13 μl, 0.1 mmol) with stirring in MeOH (2 ml) for 16 hr. This treatment results in formation of a mixture of mono- and di-BOC protected probe, **3a** and **3b**, respectively. Following solvent removal, the protected intermediates were isolated by preparative RPC18 HPLC (eluting with a gradient from 0% to 75% buffer B with a flow rate of 6 ml/min over 50 min) giving **3a** (3.6 mg, 9%, LRMS (ESI) $[M+H]^+$ calculated for

$C_{38}H_{30}NO_{11}S_2^+$: 740.13, found: 740.12) and **3b** (2.0 mg, 4%, LRMS (ESI) $[M+H]^+$ calculated for $C_{43}H_{38}NO_{13}S_2^+$: 840.18, found: 840.35) as orange-red solids. Intermediates **3a** and **3b** were then combined and treated with 4 ml of a 1:1 MeOH/TFA solution for 15 min. After solvent removal by rotary evaporation and drying in vacuo, pure SNAPF (3.5 mg, 10%) was obtained as a red-pink solid. Prepared SNAPF was solubilised in phosphate buffer (pH 7.4) with 0.1% DMF as a cosolvent and stored at −20°C in stock solutions of 1 mM for experimental use. ^{1}H NMR (400 MHz, d_6-DMSO): δ 9.29 (1H, d, J = 7.9 Hz), 9.21 (1H, d, J = 8.4 Hz), 8.34 (1H, s), 8.01 (1H, d, J = 8.6 Hz), 7.93 (1H, d, J = 9.2 Hz), 7.87 (1H, d, J = 7.8 Hz), 7.63 (1H, d, J = 9.0 Hz), 7.49–7.44 (3H, m), 7.34–7.26 (3H, m), 7.14 (2H, d, J = 6.2 Hz), 6.98–6.92 (2H, m). HRMS (ESI) $[M+H]^+$ calculated for $C_{33}H_{22}NO_9S_2^+$: 640.0731, found: 640.0722.

Neutrophil Isolation

Neutrophils were isolated by drawing venous blood from human volunteers and immediately centrifuging the blood through a density gradient at room temperature (Polymorphprep, Axis-Shield). This method separates distinct bands of mononuclear cells and polymorphonuclear leucocytes from erythrocytes. The band containing polymorphonuclear leucocytes was collected and washed twice in Hanks' balanced salt solution (HBSS), and then the cells were resuspended in phosphate buffer (pH 7.4) containing 150 mM sodium chloride and the appropriate fluorescent probes. Isolated cells were used in experiments without delay.

Macrophage Isolation

Human monocytes were isolated from donated whole blood by using a Ficoll density gradient, washed several times in HBSS, and matured into macrophages either with, for MPOhi cells, or without (for MPOlo) 500 U/ml GM-CSF as described previously [41]. MPOhi cells were cultured in serum-free medium. Murine macrophages were isolated by flushing bone marrow from femurs and tibias of donor mice and cell suspensions centrifuged through a Ficoll density gradient. Adherent bone marrow derived cells were then cultured to macrophages by adding a final concentration of 50 ng/ml M-CSF/5% fetal bovine serum to the culture medium.

Reverse Transcriptase Polymerase Chain Reaction

RNA was isolated from bone marrow-derived macrophages by standard procedures (RNEasy mini kit, QIAGEN). cDNA was then generated from the RNA by using a reverse transcriptase reaction (SuperscriptII RNase reverse transcriptase, Invitrogen). cDNA samples were amplified by PCR with primers specific for human MPO (forward 5′-ACCCCTGCCAAGCTGA-3′, reverse 5′-GGGGATATGAGTTGGACA, annealing at 53°C) and mouse β-actin (forward 5′-CCTGAGCGCAAGTACTCTGTGT-3′, reverse 5′-GCTGATCCACATCTGCTGGAA-3′, annealing at 60°C). Reverse transcriptase-PCR products were separated with agarose gel electrophoresis.

MPO Activity

Generation of HOCl by MPO was assessed by chlorination of taurine in Krebs-Henseleit (KH) buffer. Cultured cells were scraped into KH buffer containing 20 mM taurine and stimulated with a final concentration of 400 nM phorbol myristate acetate (PMA) at 37°C for 2 hr with periodic shaking. The reaction was stopped by the addition of catalase at 20 μg/ml of buffer followed by a 10 min incubation on melting ice. Cell suspensions were then centrifuged at 13,000 rpm for 5 min at 4°C, and a final concentration of 0.225 mM 5-thio-2-nitrobenzoic acid (TNB) added to the supernatant. The reaction was allowed to proceed for 5 min in the dark. Absorbance readings were measured at 412 nm for each sample, using buffer alone with TNB as a blank. Meanwhile, cell pellets were resuspended in triton homogenizing buffer, lysed by sonication for 1 min, and protein measurements were taken for each sample. Results were expressed as the percent decrease in absorbance at 412 nm from the blank sample per μg of protein.

Fluorescence Microscopy

Cells were cultured in black, clear bottomed 96-well plates (Costar). On the day of the experiment, cells were washed twice in HBSS and incubated in 0.1 M sodium phosphate buffer (pH 7.4), containing 150 mM sodium chloride and appropriate probes, with or without MPO inhibitor. Cells were incubated at 37°C in the dark for 10 min, and then prestimulation images were acquired. Cells were then stimulated with PMA at a concentration of 400 nM in the buffer and incubated, protected from light, at 37°C for a further 60 min, after which poststimulation images were obtained. Images were acquired with either a FITC (excitation 480/30 nm, emission 535/40 nm) or APC (excitation 620/60 nm, emission 700/75 nm) filter set on a Nikon Eclipse TE2000U fluorescence microscope, utilizing Spot software.

Quantification of Fluorescence

Experimental cells were cultured in black, clear-bottomed 96-well plates (Costar), washed twice with HBSS, and then incubated at 37°C in the dark in sodium phosphate buffer containing 10 μM of the indicated probes, with or without MPO inhibitor, as above. Chemical reactions to generate the ROS were performed as described previously [38] in 0.5 ml tubes and were transferred into wells of the 96-well plates. Briefly, OH· was generated by 100 μM ferrous perchlorate/1 μM H_2O_2, HOCl by addition of 10 μM NaOCl, superoxide ($O_2^{\cdot-}$) by the addition of 100 μM KO_2, H_2O_2 by addition of 100 μM H_2O_2, nitric oxide (NO) by addition of 100 μM 3-(aminopropyl)-1-hydroxy-3-isopropyl-2-oxo-1-triazene, and alkylperoxyl radical (ROO·) by addition of 100 μM 2,2′-Azobis(2-amidinopropane)dihydrochloride. Each reaction was incubated with 10 μM SNAPF. Fluorescence readings from the plates were measured on a Safire^2 plate reader (Tecan) with Magellan software. For APF, excitation and emission filters were 495 nm and 520 nm, respectively. For SNAPF, excitation and emission filters of 600 nm and 700 nm were used.

Human Atherosclerotic Tissue

Freshly excised atherosclerotic human carotid arteries were obtained from the operating theaters at Brigham and Women's Hospital, Boston, according to protocols approved by the Institutional Review Board. Carotids were either sliced thinly and then incubated with the probes at 37°C in phosphate buffer for fluorescence imaging or were frozen in OCT and sectioned into 6 μm thick slices. Frozen sections were warmed to room temperature and then incubated with 100 μl of phosphate buffer containing 10 μM probe for 1 hr, after which they were examined by fluorescence microscopy. Serial sections were stained immunohistochemically for macrophages (primary antibody anti-CD68, 1:700, DAKO) or myeloperoxidase (rabbit anti-MPO, 1:400, DAKO) with 3-amino, 9-ethyl-carbazole (AEC) as a substrate.

In Vivo Imaging

Sterile peritonitis was induced in hMPO-Tg mice by intraperitoneal injection of 1 ml of a 3% thioglycollate solution in water. After 24 hr, live mice were imaged by FRI on a Siemens BonSAI system with filters for far-red imaging (excitation 660 nm, emission 735 nm). The fluorescent probes were injected into the mice intraperitoneally, and the animals were imaged again after 1 hr. The changes in fluorescence signal intensity over baseline were quantified by region of interest (ROI) analysis with OsiriX version 2.5.1.

Statistical Analysis

Statistical significance was calculated by determining p values by using the paired t test.

ACKNOWLEDGMENTS

This work was funded by the National Heart, Lung, and Blood Institute Program for Excellence in Nanotechnology, funding number UO1 HL080731 (R.W.). We thank Dr. Galina Sukhova for samples of human atherosclerotic plaque, and we also thank Elissa Simon-Morrissey, Eugenia Shvartz, and Lindsey MacFarlane for technical assistance.

Received: July 30, 2007
Revised: October 3, 2007
Accepted: October 3, 2007
Published: November 26, 2007

REFERENCES

1. Halliwell, B. (2007). Oxidative stress and cancer: have we moved forward? Biochem. J. *401*, 1–11.
2. Bowler, R.P., and Crapo, J.D. (2002). Oxidative stress in allergic respiratory disease. J. Allergy Clin. Immunol. *110*, 349–356.
3. Bickers, D.R., and Athar, M. (2006). Oxidative stress in the pathogenesis of skin disease. J. Invest. Dermatol. *126*, 2565–2575.
4. McCord, J.M. (1974). Free radicals and inflammation: protection of synovial fluid by superoxide dismutase. Science *185*, 529–531.
5. McCord, J.M., and Day, E.D. (1978). Superoxide-dependent production of hydroxyl radical catalyzed by iron-EDTA complex. FEBS Lett. *86*, 139–142.
6. Repine, J.E., Fox, R.B., and Berger, E.M. (1981). Hydrogen peroxide kills *Staphylococcus aureus* by reacting with staphylococcal iron to form hydroxyl radical. J. Biol. Chem. *256*, 7094–7096.
7. Harrison, J.E., and Schultz, J. (1976). Studies on the chlorinating activity of myeloperoxidase. J. Biol. Chem. *251*, 1371–1374.
8. Morris, J.C. (1966). The acid ionization constant of HOCl from 5 to 35°. J. Phys. Chem. *70*, 3798–3805.
9. Hammerschmidt, S., Buchler, N., and Wahn, N. (2002). Tissue lipid peroxidation and reduced glutathione depletion in hypochlorite-induced lung injury. Chest *121*, 573–581.
10. Venglarik, C.J., Giron-Calle, J., Wigley, A.F., Malle, E., Watanabe, N., and Forman, H.J. (2003). Hypochlorous acid alters bronchial epithelial cell membrane properties and prevention by extracellular glutathione. J. Appl. Physiol. *95*, 2444–2452.
11. Hammerschmidt, S., Vogel, T., Jockel, S., Gessner, C., Seyfarth, H.J., Gillissen, A., and Wirtz, H. (2007). Protein kinase C inhibition attenuates hypochlorite-induced acute lung injury. Respir. Med. *101*, 1205–1211.
12. Wu, S.M., and Pizzo, S.V. (2001). α2-macroglobulin from rheumatid arthritis synovial fluid: functional analysis defines a role for oxidation in inflammation. Arch. Biochem. Biophys. *391*, 119–126.
13. Jasin, H.E. (1993). Oxidative modification of inflammatory synovial fluid immunoglobulin G. Inflammation *17*, 167–181.
14. Hasegawa, T., Malle, E., Farhood, A., and Jaeschke, H. (2005). Generation of hypochlorite-modified proteins by neutrophils during ischaemia-reperfusion injury in rat liver: attenuation by ischemic preconditioning. Am. J. Physiol. Gastrointest. Liver Physiol. *289*, G760–G767.
15. Malle, E., Buch, T., and Grone, H.-J. (2003). Myeloperoxidase in kidney disease. Kidney Int. *64*, 1956–1967.
16. Maruyama, Y., Lindholm, B., and Stenvinkel, P. (2004). Inflammation and oxidative stress in ESRD—the role of myeloperoxidase. J. Nephrol. *17*, S72–S76.
17. Berliner, J.A., and Heinecke, J.W. (1996). The role of oxidized lipoproteins in atherosclerosis. Free Radic. Biol. Med. *20*, 707–728.
18. Daugherty, A., Dunn, J.L., Rateri, D.L., and Heinecke, J.W. (1994). Myeloperoxidase, a catalyst for lipoprotein oxidation, is expressed in human atherosclerotic lesions. J. Clin. Invest. *94*, 437–444.
19. Hazell, L.J., Arnold, L., Flowers, D., Waeg, G., Malle, E., and Stocker, R. (1996). Presence of hypochlorite-modified proteins in human atherosclerotic lesions. J. Clin. Invest. *97*, 1535–1544.
20. Hazen, S.L., and Heinecke, J.W. (1997). 3-chlorotyrosine, a specific marker of myeloperoxidase-catalyzed oxidation, is markedly elevated in low density lipoprotein isolated from human atherosclerotic intima. J. Clin. Invest. *99*, 2075–2081.
21. Brennan, M.-L., Anderson, M.M., Shih, D.M., Qu, X.-D., Wang, X., Mehta, A.C., Lim, L.L., Shi, W., Hazen, S.L., Jacob, J.S., et al. (2001). Increased atherosclerosis in myeloperoxidase-deficient mice. J. Clin. Invest. *107*, 419–430.
22. McMillen, T.S., Heinecke, J.W., and LeBoeuf, R.C. (2005). Expression of human myeloperoxidase by macrophages promotes atherosclerosis in mice. Circulation *111*, 2798–2804.
23. Zhang, R., Brennan, M.-L., Fu, X., Aviles, R.J., Pearce, G.L., Penn, M.S., Topol, E.J., Sprecher, D.L., and Hazen, S.L. (2001). Association between myeloperoxidase levels and risk of coronary artery disease. JAMA *286*, 2136–2142.
24. Brennan, M.-L., Penn, M.S., Van Lente, F., Nambi, V., Shishehbor, M.H., Aviles, R.J., Goormastic, M., Pepoy, M.L., McErlean, E.S., Topol, E.J., et al. (2003). Prognostic value of myeloperoxidase in patients with chest pain. N. Engl. J. Med. *349*, 1595–1604.
25. Baldus, S., Heeschen, C., Meinertz, T., Zeiher, A.M., Eiserich, J.P., Munzel, T., Simoons, M.L., and Hamm, C.W. (2003). Myeloperoxidase serum levels predict risk in patients with acute coronary syndromes. Circulation *108*, 1440–1445.
26. Sugiyama, S., Kugiyama, K., Aikawa, M., Nakamura, S., Ogawa, H., and Libby, P. (2004). Hypochlorous acid, a macrophage product, induces endothelial apoptosis and tissue factor expression. Arterioscler. Thromb. Vasc. Biol. *24*, 1309–1314.
27. Hazell, L.J., and Stocker, R. (1993). Oxidation of low-density lipoprotein with hypochlorite causes transformation of lipoprotein into a high-uptake form for macrophages. Biochem. J. *290*, 165–172.
28. Goldstein, J.L., Ho, Y.K., Basu, S.K., and Brown, M.S. (1979). Binding site on macrophages that mediates uptake and degradation of acetylated low density lipoprotein, producing massive cholesterol deposition. Proc. Natl. Acad. Sci. USA *76*, 333–337.
29. Katsura, M., Fortser, L.A., Ferns, G.A., and Anggard, E.E. (1994). Oxidative modification of low-density lipoprotein by human polymorphonuclear leucocytes to a form recognized by the lipoprotein scavenger pathway. Biochim. Biophys. Acta *1213*, 231–237.
30. McMurray, H.F., Parthasarathy, S., and Steinberg, D. (1993). Oxidative modification of low-density lipoprotein by human polymorphonuclear leucocytes to a form recognized by the lipoprotein scavenger pathway. J. Clin. Invest. *92*, 1004–1008.
31. Terkeltaub, R., Banka, C.L., Solan, J., Santoro, D., Brand, K., and Curtiss, L.K. (1994). Oxidized LDL induces monocytic cell expression of interleukin-8, a chemokine with T-lymphocyte chemotactic activity. Arterioscler. Thromb. *14*, 47–53.
32. Wang, G.P., Deng, Z.D., Ni, J., and Qu, Z.L. (1997). Oxidized low density lipoprotein and very low density lipoprotein enhance expression of monocyte chemoattractant protein-1 in rabbit peritoneal exudate macrophages. Atherosclerosis *133*, 31–36.
33. Yla-Herttuala, S., Palinski, W., Butler, S.W., Picard, S., Steinberg, D., and Witztum, J.L. (1994). Rabbit and human atherosclerotic lesions contain IgG that recognizes epitopes of oxidized LDL. Arterioscler. Thromb. *14*, 32–40.
34. Stemme, S., Faber, B., Holm, J., Wiklund, O., Witztum, J.L., and Hansson, G.K. (1995). T lymphocytes from human atherosclerotic plaques recognize oxidized low density lipoprotein. Proc. Natl. Acad. Sci. USA *92*, 3893–3897.
35. Bergt, C., Fu, X., Huq, N.P., Kao, J., and Heinecke, J.W. (2003). Lysine residues direct the chlorination of tyrosines in YXXK motifs of apolipoprotein A-1 when hypochlorous acid oxidizes high density lipoprotein. J. Biol. Chem. *279*, 7856–7866.
36. Bergt, C., Pennathur, S., Fu, X., Byun, J., O'Brien, K., McDonald, T.O., Singh, P., Anantharamaiah, G.M., Chait, A., Brunzell, J., et al. (2004). The myeloperoxidase product hypochlorous acid oxidizes HDL in the human artery wall and impairs ABCA1-dependent cholesterol transport. Proc. Natl. Acad. Sci. USA *101*, 13032–13037.

37. Shao, B., Oda, M.N., Bergt, C., Fu, X., Green, P.S., Brot, N., Oram, J.F., and Heinecke, J.W. (2006). Myeloperoxidase impairs ABCA1-dependent cholesterol efflux through methionine oxidation and site-specific tyrosine chlorination of apolipoprotein A-1. J. Biol. Chem. *281*, 9001–9004.

38. Setsukinai, K., Urano, Y., Kakinuma, K., Majima, H.J., and Nagano, T. (2003). Development of novel fluorescence probes that can reliably detect reactive oxygen species and distinguish specific species. J. Biol. Chem. *278*, 3170–3175.

39. Weissleder, R., and Ntziachristos, V. (2003). Shedding light onto live molecular targets. Nat. Med. *9*, 123–128.

40. Hilderbrand, S.H., and Weissleder, R. (2007). One-pot synthesis of new symmetric and asymmetric xanthene dyes. Tetrahedron Lett. *48*, 4383–4385.

41. Sugiyama, S., Okada, Y., Sukhova, G., Virmani, R., Heinecke, J.W., and Libby, P. (2001). Macrophage myeloperoxidase regulation by granulocyte macrophage colony-stimulating factor in human atherosclerosis and implications in acute coronary syndromes. Am. J. Pathol. *158*, 879–891.

42. Test, S.T. (1991). Effect of tumor necrosis factor on the generation of chlorinated oxidants by adherent human neutrophils. J. Leukoc. Biol. *50*, 131–139.

43. Bergt, C., Marsche, G., Panzenboeck, U., Heinecke, J.W., Malle, E., and Sattler, W. (2001). Human neutrophils employ the myeloperoxidase/hydrogen peroxide/chloride system to oxidatively damage apolipoprotein A-1. Eur. J. Biochem. *268*, 3523–3531.

44. Gomes, A., Fernandes, E., and Lima, J.L. (2005). Fluorescence probes used for detection of reactive oxygen species. J. Biochem. Biophys. Methods *65*, 45–80.